Journal of Science and Transport Technology
Journal homepage: https://jstt.vn/index.php/en

System design and Flow simulation of a Blowdown Sliding-block Supersonic Wind tunnel

Vu-Hoang-Long Nguyen, Thi-Kim-Dung Hoang*
School of Mechanical Engineering, Hanoi University of Science and Technology, No 1 Dai Co Viet St., Bach Mai Ward, Hanoi 11618, Vietnam

Article info
Type of article:
Original research paper

DOI:
https://doi.org/10.58845/jstt.utt.2025.en.5.3.71-80

***Corresponding author:**
Email address:
dung.hoangthikim@hust.edu.vn

Received: 04/04/2025
Received in Revised Form: 28/06/2025
Accepted: 15/08/2025

Abstract: This study presents the design, simulation and performance evaluation of a blowdown sliding-block supersonic wind tunnel having a test section sized 20 × 20 cm, capable of operating in the range of Mach number from 2 to 4. This sliding-block mechanism allows precise control of Mach number by adjusting the nozzle throat area. A computational fluid dynamics (CFD) simulation was performed at Mach 2.5 to evaluate the flow characteristics. The 3D geometry was simplified into a 2D axisymmetric model, and a structured quadrilateral mesh was generated using ANSYS Meshing. The density-based solver in ANSYS Fluent with the RNG k-epsilon turbulence model was employed to capture supersonic flow phenomena. Results demonstrate that the system achieves the target Mach number with a relative error of less than 0.4%, indicating excellent flow quality, and no major observed shock wave. The study validates the wind tunnel's performance, providing a reliable foundation for experimental aerodynamic testing.
Keywords: ANSYS; CFD; Supersonic Wind Tunnel; Sliding-block.

1. Introduction

Supersonic wind tunnels (SSWT) are essential facilities for studying high-speed aerodynamic phenomena, typically covering a range of Mach number from 1.2 to 5. These tunnels are categorized into continuous and intermittent types, depending on their operational principles. Continuous supersonic wind tunnels provide a steady-state airflow but require high operational costs due to complex power and vacuum systems. In contrast, intermittent wind tunnels, such as blowdown, Ludwieg tube, and shock tunnels, operate in short bursts using stored high-pressure air, making them more cost-effective and structurally simpler [1]. Among them, blowdown wind tunnels are widely used due to their ability to generate high-quality supersonic flow at a lower cost than continuous tunnels [2].

Blowdown wind tunnels offer several advantages over other types. Compared to continuous tunnels, they require lower initial investment and operational costs while maintaining flexible operation through shared air supply systems. These tunnels also enable rapid establishment of test conditions, reducing the risk of model failure during operation. Additionally, compared to indraft tunnels, blowdown tunnels can achieve a wider range of Reynolds numbers at a fixed Mach number, allowing better simulation of real flight conditions [3]. Furthermore, short-duration combustion and heating tests can be conducted in these tunnels, making them suitable

for diverse applications in aerodynamics and propulsion [4].

The design of supersonic nozzles plays a crucial role in ensuring flow uniformity and performance in SSWT. Various methods have been developed for nozzle contour design, including analytical, numerical, and experimental approaches. One of the foundational design techniques is the method of characteristics (MOC), which is widely used to generate axisymmetric and two-dimensional nozzle contours for achieving uniform supersonic flow [5]. Early study by Liepman [6] proposed an analytical approach for designing two-dimensional asymmetric curved nozzles, which remains relevant in modern supersonic wind tunnel applications. Additionally, Pope's extensive research on high-speed wind tunnel testing provides valuable insights into the challenges associated with supersonic nozzle and diffuser design [7].

The development of blowdown supersonic wind tunnels has been extensively studied over the years. Early studies focused on startup characteristics and nozzle contour optimization [8], while more recent advancements have improved diffuser efficiency, flow uniformity, and computational modeling techniques [9,10]. Additional studies on supersonic tunnel aerodynamics, diffuser performance, and high-speed flow characteristics have been documented by researchers such as Anderson [11] and Christopher [12].

Despite the advantages of sliding-block blowdown SSWT in adjusting test Mach numbers, most existing designs lack detailed analysis of flow quality within the test section. In particular, there is a shortage of data evaluating how changes in the sliding-block position affect flow uniformity and shock wave behavior.

Previous studies on blowdown wind tunnels have mainly focused on structural design or theoretical estimation of Mach number distributions [13, 14]. However, few works provide in-depth CFD-based analysis of flow quality metrics such as Mach number uniformity, velocity gradients, or thermal behavior in the test section. In particular, diffuser optimization for stable pressure recovery is often overlooked.

This study builds upon previous research by designing a blowdown SSWT system incorporating a sliding-block nozzle, which enables variable Mach number operation. The system is designed to achieve a test section sized 20 × 20 cm having Mach numbers from 2 to 4. The sliding-block nozzle dynamically adjusts the throat area to achieve different Mach numbers, while the adjustable diffuser ensures efficient pressure recovery. The computational simulations at Mach 2.5 are caried out to evaluate flow quality, pressure distribution, and shockwave behavior. The results provide valuable insights into optimizing wind tunnel designs for improved performance and cost efficiency.

2. Methodology

Starting compression ratio depends on the test section Mach number. The higher the Mach number, the higher the inlet pressure is required. Therefore, it is more effective to start from lower Mach number, then adjust to higher one, which can be solved by an adjustable nozzle. The suitable Mach range is from 2 to 4. The idea is to use Liepman's wind tunnel, which has an adjustable sliding-block so that the ratio of the area of first throat and the area of test section can be changed, which leads to the change in test section Mach number (Fig.1) [6].

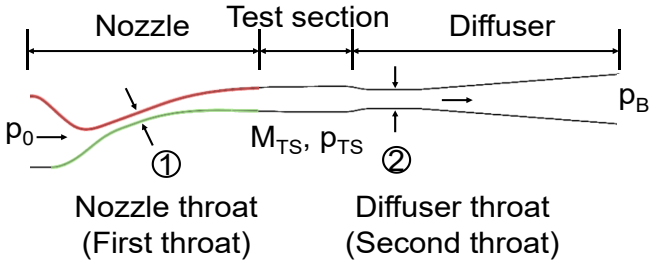

Fig 1. Schematic of the sliding-block wind tunnel with a diffuser

In the case where the test section is directly at the exit, namely "free jet wind tunnel", the pressure ratio between inlet pressure and outlet

pressure is calculated using isentropic flow relation, which leads to a very high pressure required at the inlet. Thus, there should be a diffuser, which can create shockwaves to increase pressure exiting the wind tunnel. Namely, the diffuser decreases the pressure in the test section, so that this pressure ratio or compression ratio can be reduced

$$\lambda = \frac{p_o}{p_b} = \frac{p_o}{p_{TS}} \frac{p_{TS}}{p_b} \quad (1)$$

where p_0 is inlet pressure; p_b is outlet pressure; p_{TS} is pressure in test section (Fig.1).

The compression ratio λ between the inlet and exit pressure in order to start the wind tunnel in case a diffuser is used is presented as (Fig.2).

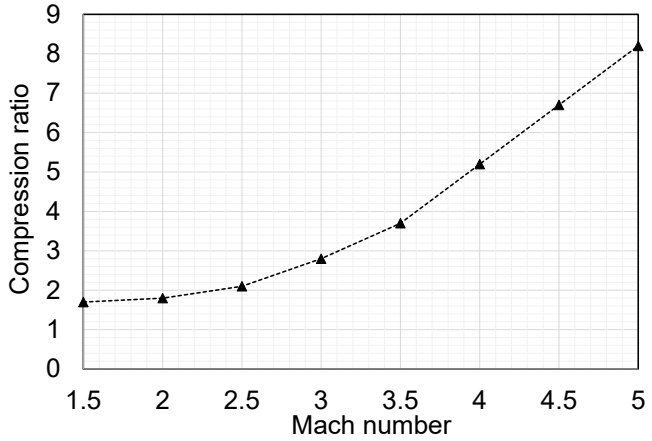

Fig 2. Relationship between minimum startable pressure and Mach number

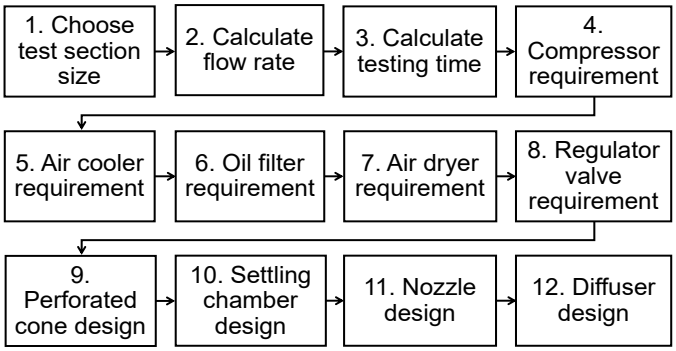

Fig 3. Workflow of designing a blowdown supersonic wind tunnel

As mentioned before, the overall SSWT system contains several sub-systems and components, the design workflow is as follows (Fig.3). Firstly, we need to specify the test section size that is suitable for the budget and test demand, then evaluate the requirement of the air compression system, and finally, ensure that the nozzle and diffuser design make the wind tunnel be able to start.

3. Design of Mach 2.5 supersonic wind tunnel

The following section outlines general guidelines to follow in order to design and evaluate a blowdown supersonic wind tunnel system (Fig. 3).

3.1. Choose test section size

The size of the test section directly affects the flow quality and the capability of aerodynamic testing. Common supersonic wind tunnel test section sizes range from 10×10 cm to 30×30 cm, depending on research requirements. Considering factors such as flow uniformity, diffuser efficiency, and cost constraints, a 20×20 cm test section is selected. This size provides a balance between achieving stable supersonic flow, accommodating small-scale models, and minimizing energy losses while ensuring practical experimental conditions.

3.2. Calculate flow rate

The airflow rate through the wind tunnel is one of the primary considerations in sizing both the wind tunnel and the associated equipment.

To achieve Mach 2.5 in a test section of 20×20 cm, the airflow rate along the wind tunnel is calculated using the following equation

$$\dot{w} = 0.0402 \frac{p_t A_1^*}{\sqrt{T_t}} \quad (2)$$

where A_1^* is area of first throat; T_t is total temperature.

As p_t=p_0 is the minimum operating pressure from Fig.1, the relationship between the area of the throat, A*, the area of test section, A, and the Mach number is operated by Hugoniot theorem as follows

$$\frac{A}{A^*} = \frac{1}{M} \left(\frac{1 + \frac{\gamma - 1}{2} M^2}{\frac{\gamma + 1}{2}} \right)^{\frac{\gamma+1}{2(\gamma-1)}} \quad (3)$$

For the total temperature, T_t, equals 300K, the relation between flow rate and Mach number is

presented in Fig. 4.

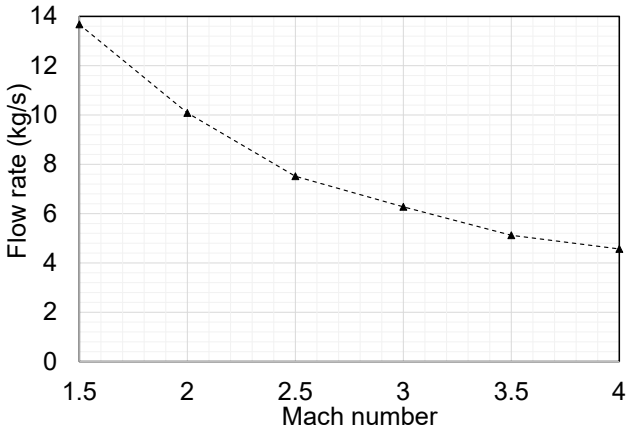

Fig 4. Relationship between flow rate and Mach number

3.3. Compression evaluation

The run time for blowing down a tank under constant mass flow rate conditions is calculated as follows

$$t = \frac{V}{A^*}\frac{\sqrt{T_t}}{T_i}\frac{p_i}{p_t}\left[1-\left(\frac{p_f}{p_i}\right)^{\frac{1}{n}}\right] \quad (4)$$

where V is tank's volume; p_i, p_f is initial pressure and final pressure of the tank respectively; T_i is initial temperature.

For $p_f=1.5p_t$ is the final pressure after the tank is fully exhausted after 40 seconds, given the tank's volume is V=20 cubic meter, the maximum initial pressure of the tank p_i is

$$p_i=1576063\text{Pa}=15.55\text{atm} \quad (5)$$

In order to increase the tank pressure from 1 atm to 15.5 atm in 0.5 hours for fast preparation time, the compressor flow rate is calculated using the following equation

$$Q=\frac{V}{14.7t}(p_i-1) \quad (6)$$

Therefore, the minimum flow rate required for the compressor is

$$Q_{min}=415\,m^3/h \quad (7)$$

3.4. Compressed air system

The compressed air system must ensure high-quality airflow before entering the wind tunnel to maintain accurate flow conditions. Air cooler, oil filter, air dryer, and pressure regulator must meet the requirement of flow rate and other specialized specifications as in Table 1.

Table 1. Compressed air system's components

Equipment	Function Description	Key Specifications
Air Cooler	Reducing the compressed air temperature to prevent thermal effects on flow properties.	Heat exchanger type; reduces temperature from ~150°C to below 40°C.
Oil Filter	Removing residual oil particles from the compressor to ensure clean, contaminant-free airflow.	0.01-micron coalescing filter.
Air Dryer	Eliminating moisture from compressed air to prevent condensation that could disrupt supersonic flow.	Desiccant type; dew point -40°C.
Regulator Valve	Controlling inlet pressure to maintain consistent and stable flow conditions in the test section.	High-pressure precision regulator; range 0–20 bar, accuracy ±0.1 bar.

3.5. Wide angle diffuser calculation

The gas flow needs to be stabilized before entering the air duct. There are two processes: (1) passing through a diffuser using a perforated cone, to expand the gas flow to a diameter equivalent to the size of the settling chamber and (2) passing through a settling chamber with mesh panels inside to reduce gas flow turbulence as seen in Fig.5.

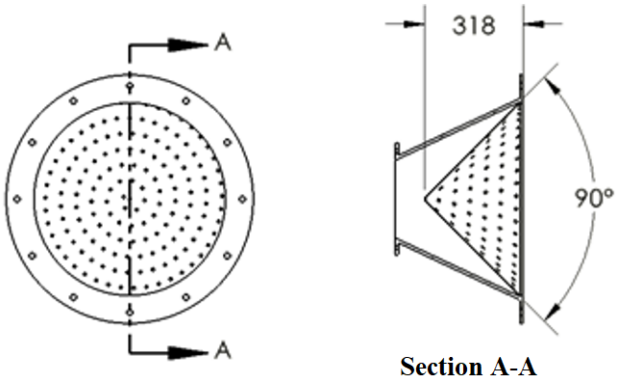

Fig 5. Design of the wide-angle diffuser

Main technical parameters of the gas diffuser mesh are calculated in accordance to Pope [7] (Fig.6).

Density of perforations: 15 - 40% of the surface area,

Hole diameter: 3 - 8 mm,

Distance from the perforated cone to the screen: 0.5 - 1.0 time the chamber diameter.

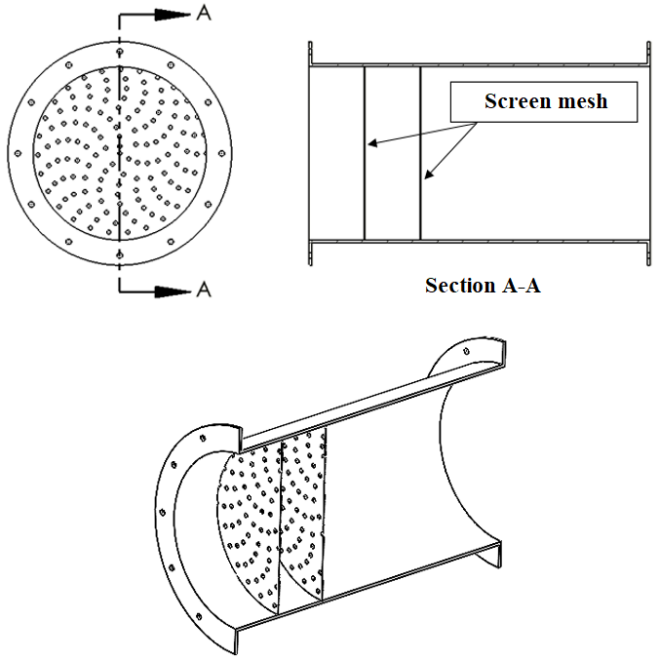

Fig 6. Design of the settling chamber

3.6. Nozzle design

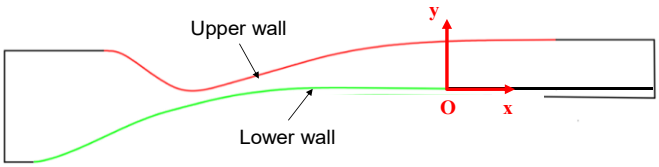

Fig 7. Lower wall can slide along x-axis

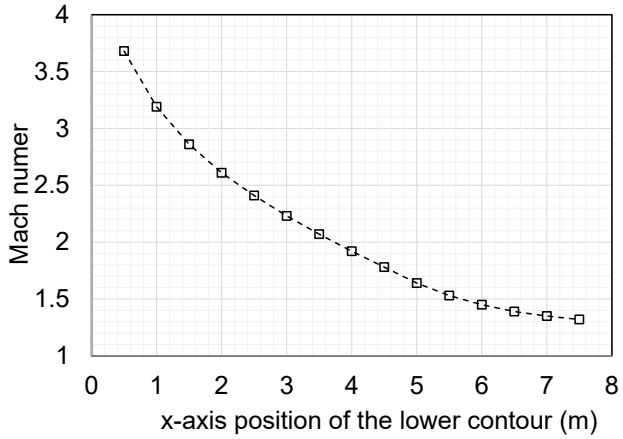

Fig 8. Lower wall position via Mach number [6]

According to Liepman [6] study, to design the profile of aerodynamic tubes on asymmetric sound, fundamental procedures are needed. The lower wall profile changes the position relative to the x-axis, changing the ratio between the throat and test section area, thereby changing the test Mach number. Basically, as the slider moves further to the right, this area ratio increases, leading to a decrease in Mach number. According to the original design, the change in slider position and the output Mach number are as follows (Fig.7-8).

3.7. Diffuser design

The overall configuration of the diffuser has not been standardized, and many studies have been conducted to optimize parameters such as the convergence angle as well as the length of the diffuser throat. Convergence angles are angles between the test section and the diffuser throat. This angle has been tested from as small as 30 degrees or larger, with diffuser throat lengths ranging from 0 to 10 times the length of the test section. However, the results are not conclusive, so adjustments need to be made to suit the system. In many cases, ultrasonic wind tunnels use a second adjustable throat diffuser to optimize the diffusion process.

The air flow is decelerated and gradually increased in pressure to the ambient pressure through the diffuser. The screw mechanism is used to adjust the position of the rollers in contact with the diffuser.

The profile of the diffuser can be changed. The goal is to gradually reduce the second throat size at the diffuser to a suitable value to optimize the inlet pressure ratio for the air duct. The relation between the area of second throat and the area of test section is described in the equation below

$$\frac{A_2^*}{A_{TS}} = \frac{(5+M)^{0.5}(7M^2-1)^{2.5}}{216M^6} \quad (8)$$

where A_2^* is the diffuser throat area; A_{TS}=400 cm^2 is the area of test section.

The relationship between the second throat area and Mach number is presented in the following graph (Fig.9).

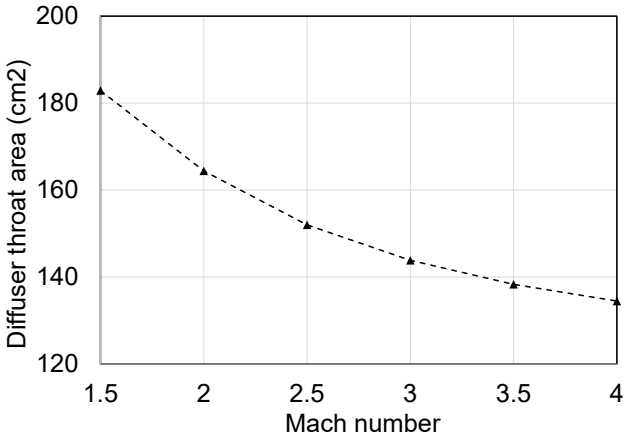

Fig 9. Throat 2 area via Mach number

4. Results and Discussion

4.1. Overall Mach 2.5 configuration

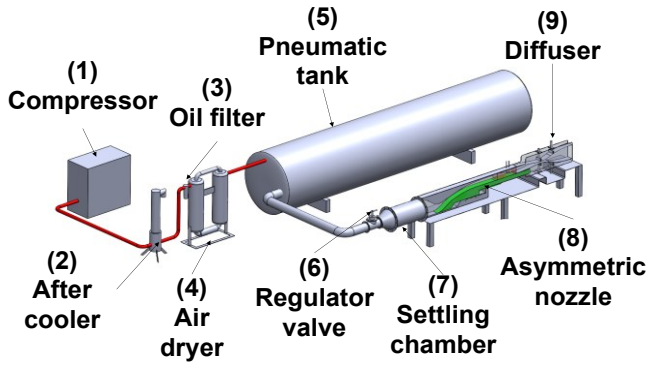

Fig 10. The overall designed system

The entire designed system is shown in Fig.10. The sliding-block supersonic wind tunnel model was configured to achieve test section Mach 2.5 by positioning the sliding-block accordingly. Additionally, the second throat of the diffuser was adjusted to match the expected Mach 2.5 conditions.

To efficiently evaluate the performance of the wind tunnel design, the simulation was conducted at Mach 2.5, representing a mid-range condition within the full operational Mach number range of 2 to 4. This approach was chosen to reduce computational cost and time while still capturing the essential aerodynamic behaviors. Simulating at Mach 2.5 allows for the simultaneous assessment of several key parameters:

(1) The geometric position of the sliding-block for throat adjustment,

(2) The resulting Mach number distribution and flow uniformity in the test section,

(3) The effectiveness of the diffuser geometry in decelerating supersonic flow and managing shock wave behavior.

As Mach 2.5 is a representative point within the design envelope, ensuring stable and uniform flow under this condition provides a reliable basis to infer the performance at other Mach numbers through geometric similarity and theoretical scaling.

4.2. Nozzle flow simulation for Mach 2.5 configuration

To simplify the computational model, the 3D geometry was converted into a 2D model using SolidWorks, maintaining the key dimensions: 0.2 m test section height and a 7.5 m total wind tunnel length (Fig.11).

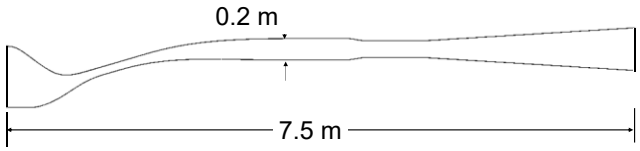

Fig 11. 2D model of the nozzle

a) Mesh at the nozzle

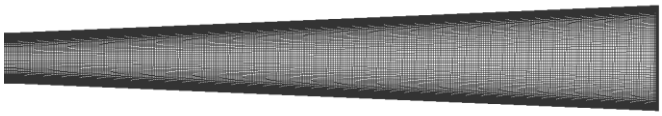

b) Mesh at the diffuser

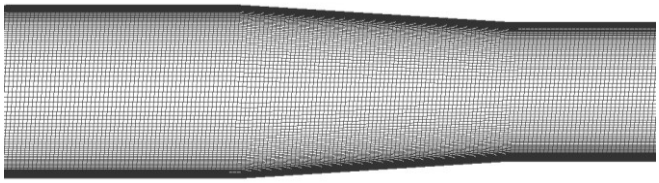

c) Mesh at the test section

Fig 12. Nozzle 2D meshing

The meshing was generated in ANSYS Meshing, utilizing quad elements with face meshing enabled. The mesh element size ranged from 0.1 mm (minimum) to 5 mm (maximum), with boundary layer cells of 0.15 mm height to capture

near-wall effects accurately (Fig.12). Boundary conditions were applied, including inlet, wall, and outlet definitions.

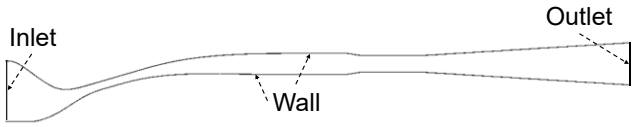

Fig 13. Boundary conditions

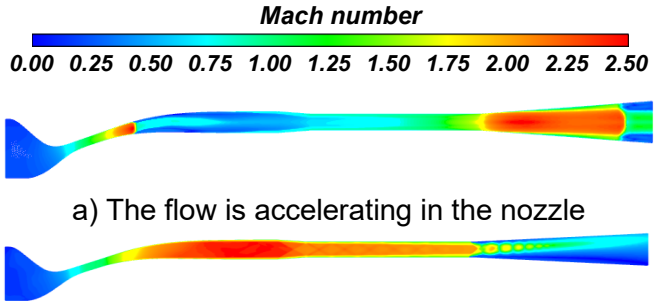

a) The flow is accelerating in the nozzle

b) The flow is completely accelerated in the test section and decelerated in the diffuser

Fig 14. Result convergent process

The simulation was conducted in ANSYS FLUENT using the density-based solver in transient mode, with the energy equation enabled to account for temperature variations. Several turbulence models were considered, including SST k-ω, Spalart–Allmaras, and RNG k-ε. The SST k-ω model offers high accuracy near walls but requires fine near-wall meshing, increasing computational cost. The Spalart–Allmaras model is efficient but less reliable for internal shock flows. The RNG k-ε model was selected as a balanced choice, capable of capturing flow separation, shock-induced effects, and streamline curvature with reasonable computational demand. It has been validated in previous studies for internal compressible flows and showed good performance in predicting flow uniformity and Mach number stability in the test section. Grid independence was also confirmed using this model, supporting its suitability for simulating supersonic flows in the present wind tunnel design. The boundary conditions were: (1) Pressure inlet is 2.5 atm (2) Pressure outlet is 1 atm (3) Operating pressure is 0 atm (Fig. 13).

The simulation converged after 75,000 iterations, with a total runtime of 8 hours on an Intel Xeon Processor E5-2678V3 (24 cores, 48 threads) with 32GB RAM (Fig. 14).

To ensure the reliability of the CFD simulation, a grid independent study was conducted using four mesh densities: 50,000; 100,000; 150,000; and 250,000 elements (Fig.15).

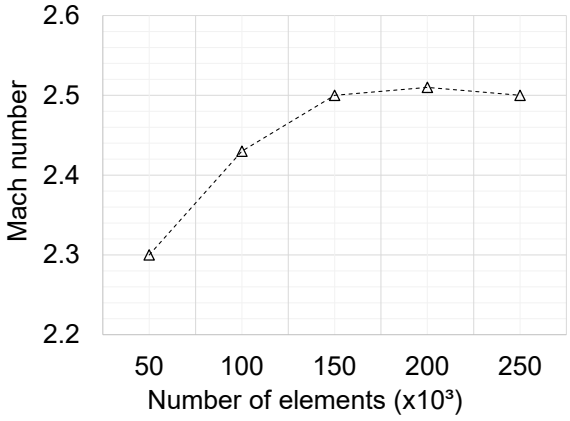

Fig 15. Mesh convergence analysis

The flow field in the test section was monitored to assess the sensitivity of the results to grid resolution. The Mach number and pressure distributions showed significant changes when increasing the mesh size from 50,000 to 100,000 elements. However, the results between 150,000 and 250,000 elements differed by less than 0.2%, indicating that the solution had converged with respect to grid size. Therefore, the mesh with 150,000 elements was considered sufficiently accurate and was selected for all subsequent simulations to balance accuracy and computational cost.

The simulation results reveal a series of weak oblique shockwaves forming in the diffuser section, downstream of the test section (Fig.16). These shock structures, often referred to as a shock train, are typical in supersonic deceleration zones and indicate the gradual reduction of flow Mach number from supersonic to near-sonic conditions. The presence of these shocks arises due to pressure mismatch between the supersonic core flow and the downstream subsonic or ambient pressure environment.

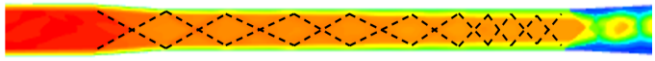

Fig 16. Shock waves pattern

Importantly, the shock waves remain

confined within the diffuser and do not propagate upstream into the test section. This ensures that the core flow remains uniform and undisturbed, preserving high-quality flow conditions for aerodynamic testing. Each shock wave contributes to a local increase in static pressure and a corresponding loss in total pressure. The smooth transition and controlled placement of the shocks demonstrate that the diffuser geometry has been effectively designed to accommodate pressure recovery without inducing flow separation or instability.

Overall, the shock wave pattern observed validates the diffuser's ability to manage supersonic deceleration while maintaining test section flow quality a critical aspect in blowdown-type SSWT.

The velocity, temperature and Mach number along α line is consequently presented in Fig.17.

Fig 17. α line position

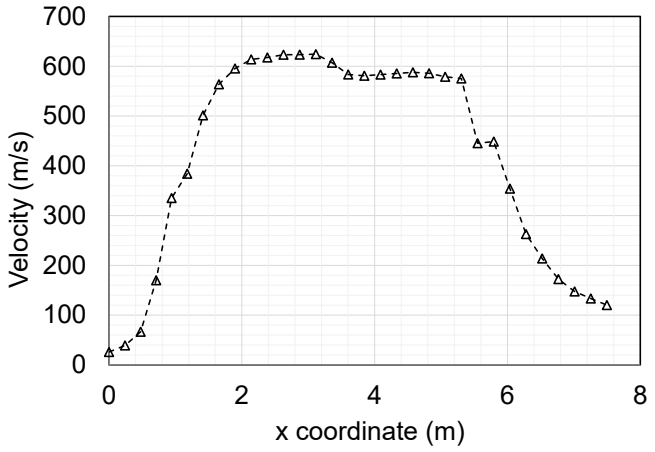

Fig 18. Velocity distribution

The velocity profile along the x-direction shows a gradual increase as the flow accelerates through the converging section, reaching a maximum velocity of approximately 600 m/s at the test section (Fig.18). This corresponds to the supersonic regime, confirming that the nozzle is effectively accelerating the flow. A sudden velocity drop occurs around x = 5.5 m, indicating a shock wave formation in the diffuser. After the shock, the velocity decreases significantly as the flow transitions back to subsonic conditions.

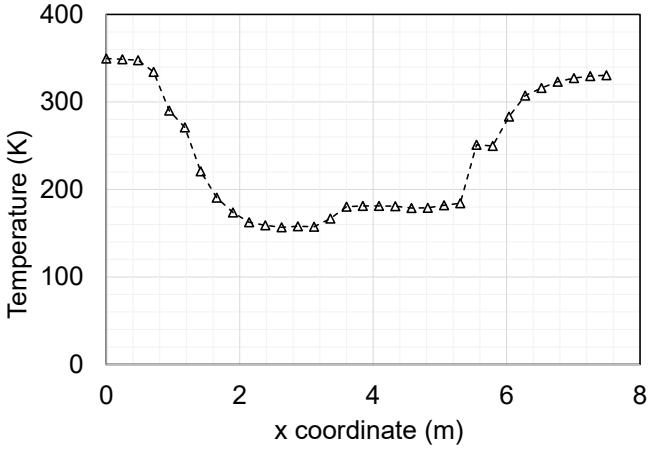

Fig 19. Temperature distribution

The temperature distribution follows an inverse relationship with velocity, decreasing as the flow accelerates through the convergent-divergent section (Fig.19).

At the test section, the temperature reaches its lowest value, around 120 K, due to the high-speed expansion of the flow. A sharp temperature rise occurs at x = 5.5 m, corresponding to the shock wave location in the diffuser, where kinetic energy converts back into thermal energy. This confirms that a normal shock is present, significantly increasing entropy and reducing flow efficiency. A gradual increase in temperature in the subsonic region indicates heat recovery in the diffuser.

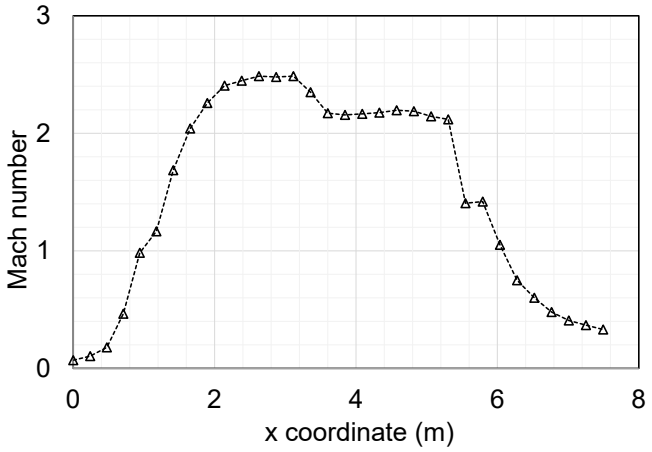

Fig 20. Mach number distribution

The Mach number profile clearly illustrates the transition from subsonic to supersonic flow through the nozzle, reaching a peak of Mach 2.5 in

the test section (Fig.20). This verifies that the nozzle design effectively produces the desired supersonic conditions. However, at x = 5.5 m, a sudden Mach number drop occurs, signifying a normal shock wave inside the diffuser. Beyond this point, the flow decelerates into the subsonic regime, confirming the presence of shock-induced losses. The downstream Mach number remains relatively low, suggesting that the diffuser is not fully effective in converting dynamic pressure back into static pressure.

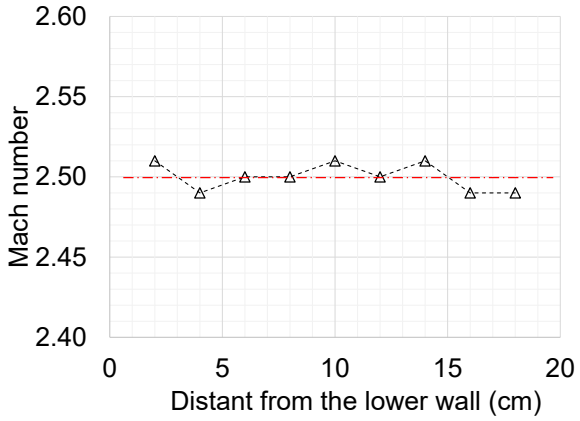

Fig 21. Test section flow uniformity

The flow within the test section is highly uniform and stable. The average Mach number across the test section is approximately 2.5, with a relative deviation of less than 0.4%, indicating excellent agreement with the target value (Fig.21). The flow remains symmetrical and free from large-scale disturbances, which is essential for accurate aerodynamic testing.

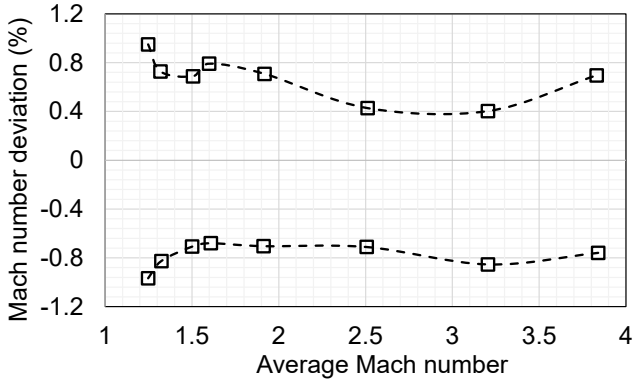

Fig 22. Experimental Mach number deviation data [8]

Although experimental studies on asymmetric sliding block nozzles are limited, the Mach number distribution along the test section is compared with Liepman's experimental results [8]. According to Liepman's experimental data, for a Mach number of 2.5, the test section Mach number deviation ranges from 0.4% to 0.6% (Fig. 22); therefore, these CFD results are considered validated.

5. Conclusion

This study successfully designed a blowdown sliding-block SSWT tailored for a test section size of 20×20 cm and a range of Mach numbers from 2 to 4, integrated with a geometrically sliding-block nozzle.

A unified simulation framework that simultaneously addresses Mach control, flow uniformity, and shock wave management was provided. Results show that the average Mach number across the test section is approximately 2.5, with a relative deviation of less than 0.4%. No significant shock waves are observed within the test section; instead, a weak shock train forms downstream in the diffuser region. This indicates that the diffuser effectively manages pressure recovery without compromising the upstream flow quality. The velocity, temperature, and Mach number distributions aligned well with theoretical expectations.

Future work will focus on extending the simulation to full 3D geometry to capture crossflow effects, and on conducting experimental validation using pressure sensors and optical flow diagnostics to verify simulation accuracy.

Symbols

p_0 : pressure inlet of the wind tunnel, Pa
p_b : pressure behind the wind tunnel, Pa
p_t : pressure to run the wind tunnel, Pa
p_i : maximum initial pressure of the tank, Pa
p_f : final pressure of the tank, Pa
M : Mach number
λ : compression ratio
A^* : area of the throat, m^2
$\dot{w}$: flow rate along the wind tunnel,
t : testing time of the wind tunnel, s
V : tank's volume, m^3
Q : compressor's flow rate, m^3/h

Q_{min} : minimum flow rate required for the compressor, m^3/h

Subscripts

1 : nozzle throat (First throat)
2 : diffuser throat (Secon throat)
TS : test section

References

[1]. V.S.D. Thampuratty, B. Nithin, et al. (2022). Concept Design and Development of Supersonic Wind Tunnel. *Journal of Emerging Technologies and Innovative Research (JETIR)*, 9(6), 209-217.

[2]. J.D. Anderson, Jr. (2003). Modern Compressible Flow: With Historical Perspective, 3rd ed. *McGraw-Hill, New York*.

[3]. B. Ilić, M. Milosavljević, J. Isaković, M. Miloš. (2016). Stagnation Pressure Transient Control in a Supersonic Blowdown Wind Tunnel Test Facility. *Materials Today: Proceedings*, 3(4), 987-992. https://doi.org/10.1016/j.matpr.2016.03.034

[4]. B.K. Bharath. (2015). Design and Fabrication of a Supersonic Wind Tunnel. *International Journal of Engineering and Applied Sciences (IJEAS)*, 2(5), 103-107.

[5]. P.A. Thompson. (1972). Compressible-Fluid Dynamics. *McGraw-Hill, New York, USA*.

[6]. H.P. Liepman. (1953). An Analytic Design Method for a Two-Dimensional Asymmetric Curved Nozzle. Technical Report. *University of Michigan.*

[7]. A. Pope. (1954). High-Speed Wind Tunnel Testing. *John Wiley & Sons, New York*.

[8]. H.P. Liepman, et al. (1955). Development of a variable Mach number Sliding-block Nozzle and Evaluation in the Mach 1.3 to 4.0 Range. WADC Technical Report No. 55-88. *University of Michigan*.

[9]. S. Mittal, S. Yadav. (2001). Computation of flows in supersonic Wind-tunnels. *Computer Methods in Applied Mechanics and Engineering*, 191(6-7), 611-634. doi.org/10.1016/S0045-7825(01)00305-X

[10]. Sidharth GS, J. Hilker. (2024). The Effects of Diffuser Throat Design for a Supersonic Indraft Wind Tunnel. *AIAA Journal*, 1-11. doi.org/10.2514/6.2024-85194

[11]. J.D. Anderson. (2017). Fundamentals of Aerodynamics, 6th ed. *McGraw-Hill, New York*.

[12]. C.J. Roy, F.G. Blottner. (2006). Review and assessment of turbulence models for hypersonic flows. *Progress in Aerospace Sciences*, 42(7-8), 469-530. doi.org/10.1016/j.paerosci.2006.12.002

[13]. J.V. Chopade, V. Kshirsagar. (2018). Aerodynamics of High Performance Vehicles. *International Research Journal of Engineering and Technology (IRJET)*, 5(3), 2182-2186.

[14]. R.D. Mehta, P. Bradshaw. (1979). Design Rules for Small Low Speed Wind Tunnels. *The Aeronautical Journal*, 83(827), 443-453. doi: 10.1017/S0001924000031985